Arrangement of photosystem II supercomplexes in crystalline macrodomains within the thylakoid membrane of green plant chloroplasts

Boekema, EJ; van Breemen, JFL; van Roon, H; Dekker, JP; Dekker, Jan P.

Published in:
Journal of Molecular Biology

DOI:
10.1006/jmbi.2000.4037

Publication date:
2000

doi:10.1006/jmbi.2000.4037 available online at http://www.idealibrary.com on IDEAL® J. Mol. Biol. (2000) 301, 1123–1133

JMB

Arrangement of Photosystem II Supercomplexes in Crystalline Macrodomains within the Thylakoid Membrane of Green Plant Chloroplasts

Egbert J. Boekema[1]*, Jan F. L. van Breemen[1], Henny van Roon[2] and Jan P. Dekker[2]

[1]*Department of Biophysical Chemistry, Groningen Biomolecular Sciences and Biotechnology Institute University of Groningen Nijenborgh 4, 9747 AG Groningen, The Netherlands*

[2]*Faculty of Sciences, Division of Physics and Astronomy Vrije Universiteit, De Boelelaan 1081, 1081 HV Amsterdam The Netherlands*

**Corresponding author*

The chloroplast thylakoid membrane of green plants is organized in stacked grana membranes and unstacked stroma membranes. We investigated the structural organization of Photosystem II (PSII) in paired grana membrane fragments by transmission electron microscopy. The membrane fragments were obtained by a short treatment of thylakoid membranes with the mild detergent *n*-dodecyl-α,D-maltoside and are thought to reflect the grana membranes in a native state. The membranes frequently show crystalline macrodomains in which PSII is organized in rows spaced by either 26.3 nm (large-spaced crystals) or 23 nm (small-spaced crystals). The small-spaced crystals are less common but better ordered. Image analysis of the crystals by an aperiodic approach revealed the precise positions of the core parts of PSII in the lattices, as well as features of the peripheral light-harvesting antenna. Together, they indicate that the so-called C_2S_2 and C_2S_2M supercomplexes form the basic motifs of the small-spaced and large-spaced crystals, respectively. An analysis of a pair of membranes with a well-ordered large-spaced crystal reveals that many PSII complexes in one layer face only light-harvesting complexes (LHCII) in the other layer. The implications of this type of organization for the efficient transfer of excitation energy from LHCII to PSII and for the stacking of grana membranes are discussed.

Keywords: photosystem II; electron microscopy; two-dimensional crystals; thylakoid membrane; grana stacking

Introduction

A key role in the energy-conserving mechanisms of green plants is played by photosystem II (PSII). Its major task is to use light energy for the reduction of plastoquinone, the oxidation of water and the formation of a transmembrane pH gradient. It consists of at least 25 different types of protein subunits (Hankamer *et al.*, 1997a), many of which are bound to the thylakoid membrane. Some subunits are involved in the capturing of solar energy and the regulation of the energy flow, others are directly or indirectly responsible for the photochemistry, including the oxidation of water to molecular oxygen.

The central part of PSII is formed by the so-called core complex. This structure binds about 40 chlorophyll *a* molecules and is responsible for all electron transfer reactions in PSII, including the formation of oxygen. There is overwhelming evidence that the PSII core complex is organized as a dimer in the stacked, appressed regions of the thylakoid membrane. The structure of the PSII core complex without the CP43 subunit has recently been determined at 8 Å resolution by electron crystallography on two-dimensional crystals (Rhee *et al.*, 1998).

The dimeric PSII core complex is surrounded by the peripheral antenna, which in green plants and algae consists of an unknown structure of several light-harvesting complex II (LHCII) proteins that together bind a large number of chlorophyll *a*, chlorophyll *b* and carotenoid (xanthophyll) molecules. Per PSII dimer, the total number of chlorophyll molecules bound in the peripheral antenna is

Abbreviations used: PS, photosystem; LHC, light-harvesting complex; α-DM, *n*-dodecyl-α,D-maltoside.

E-mail address of the corresponding author: boekema@chem.rug.nl

0022-2836/00/051123–11 $35.00/0

usually about 350-400, which implies that *in vivo* about 80 % of the sunlight directed to PSII will be absorbed by its peripheral antenna. The structure of the major (trimeric) LHCII complex is known at 3.4 Å resolution (Kühlbrandt *et al*., 1994).

Supercomplexes of PSII and LHCII have recently been isolated by mild detergent treatment of thylakoid membranes and structurally characterized by electron microscopy at about 2 nm resolution (e.g. see Boekema *et al*., 1995, 1998, 1999a,b; Nield *et al*., 2000). These supercomplexes were found to be very heterogeneous with respect to their LHCII subunits. The basic unit is the so-called C_2S_2 supercomplex (Boekema *et al*., 1998, 1999a,b), in which the central dimeric PSII core part (C_2) is surrounded by two symmetry-related structures consisting of one LHCII trimer (abbreviated S, for strongly attached), one CP26 monomer and one CP29 monomer. The C_2S_2 supercomplex can at each side bind one additional monomeric LHCII complex (CP24) and two additional LHCII trimers (abbreviated M and L, for moderately and loosely bound, respectively) at two different positions. Apart from the basic C_2S_2 supercomplex, only the C_2S_2M supercomplex was found to be quite common after isolation (Boekema *et al*., 1999a,b). The fact that only small numbers of particles with more than three LHCII trimers were found raised the question of whether they were too fragile to isolate. However, many C_2S_2M particles were found to occur in even larger associations, the so-called megacomplexes, in which two C_2S_2M supercomplexes associate to each other with both M-subunits at the interface (Boekema *et al*., 1999a). Two types of C_2S_2M megacomplexes were observed, differing by an approximately 7.5 nm translational shift of one of the C_2S_2M units. In both associations, an additional binding of an L-type trimer is not possible, indicating that the association between PSII and LHCII is intrinsically heterogeneous.

Although it is now quite clear that the C_2S_2 and/or C_2S_2M supercomplex forms the basic unit of PSII in at least a large part of the thylakoid membranes (e.g. see Nield *et al*., 2000; van Roon *et al*., 2000), it is not clear at all how these supercomplexes make up the complete membrane and how they connect to the LHCII that is not present in these complexes. Biochemical data have revealed that there should be about eight trimeric LHCII complexes per PSII dimer (Peter & Thornber, 1991). In addition, it is not clear which role the PSII-LHCII supercomplexes play in the stacking process. In the presence of divalent cations, the thylakoid membranes segregate into two structurally different components. Appressed membranes form stacks of several (up to dozens) membranes (grana membranes), which are connected by non-appressed membranes (stroma membranes) in a continuous way (reviewed by Anderson, 1999).

The ultrastructure of the intact membrane has been studied intensively in the past, mainly to address questions about the localization of the various components within the stacked and unstacked parts, and of the changes during unstacking (Staehelin, 1976), but at the time of these investigations there were no detailed data available about the PSII structure. Although it could be proven that the structures protruding from an almost flat background originated from the extrinsic parts of the PSII core structure (Seibert *et al*., 1987), no detailed concept could be formulated about the overall structure in the membrane. Only some ''hard facts'' could be deduced, such as the lattice parameters, in cases where the PSII complexes were shown to be present in ordered arrays (Miller, 1976; Simpson, 1978).

Recently, we have described the isolation and purification of inside-out paired grana membranes, obtained after partial solubilization of spinach chloroplasts with *n*-dodecyl-α,D-maltoside (α-DM, Van Roon *et al*., 2000). They frequently show macrodomains with a substantial amount of ordering. The lattice of the most dominant type of crystal is strongly reminiscent of those studied by freeze-etching of native membranes (Simpson, 1978). Here, we describe an analysis of the crystalline membrane fragments by electron microscopy using negatively stained specimens and image reconstruction techniques. With these techniques, a higher resolution can be achieved than with the previously applied freeze-fracture and freeze-etch techniques, while in addition information is gained concerning positioning of the particles in opposing membrane layers. We found two types of simultaneously existing lattices, the most abundant type of lattice is very likely composed of the C_2S_2M PSII-LHCII supercomplex, the other of the C_2S_2 PSII-LHCII supercomplex. We also show that in many cases a supercomplex in one layer faces only LHCII in the opposite layer.

Results

Grana membrane fragments

Incubation of thylakoid membranes from spinach with α-DM in the presence of 5 mM $MgCl_2$ resulted in a selective solubilization of the non-stacked, stromal parts of the membrane (van Roon *et al*., 2000). Under these conditions, the stacked grana membranes remained intact and could be separated from the solubilized protein complexes of the stroma membranes and the grana margins by a single gel-filtration chromatography step. The membranes were shown to consist of two membrane layers with an average diameter of 360 nm (van Roon *et al*., 2000), and to have polypeptide and pigment compositions that are very similar to those of the well-characterized PSII membranes prepared with Triton X-100 (Berthold *et al*., 1981).

The lumenal exposed, hydrophilic parts of PSII core complexes are clearly visible on electron microscopy images of negatively stained paired grana membranes (Figures 1 and 2), regardless of whether these complexes are randomly oriented in

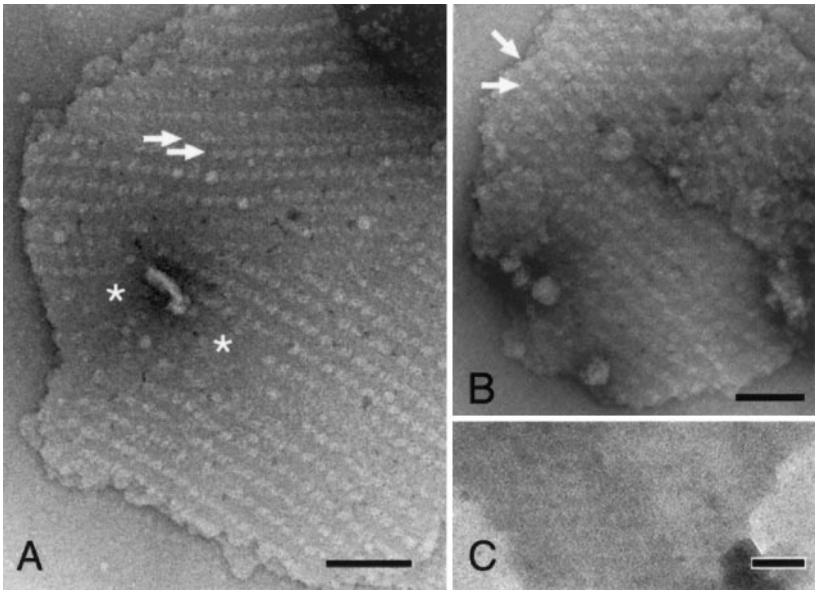

Figure 1. A gallery of large, paired inside-out grana membranes showing a semi-crystalline arrangement of PSII supercomplexes into macrodomains with a spacing of 26.3 nm between rows of PSII supercomplexes (large-spaced crystals). (a) and (b) Membranes negatively stained with 2% (w/v) uranyl acetate; (c) a frozen-hydrated, unstained fragment. Asterisks mark areas with a very smooth membrane surface, where PSII is largely absent. The two arrows in (a) point to rows of PSII supercomplexes with non-overlapping core parts; the lower row belongs to the lower membrane layer, which faces the carbon support film, and which is overall slightly more strongly stain-embedded; the two arrows in (b) indicate directions of rows from two layers differing by 45°. The space bars represent 100 nm.

the membrane, or in a semi-regular lattice. The easy detection is made possible by the fact that the peripheral antenna of PSII, composed of trimeric and monomeric LHCII, is only 6 nm thick and very flat (Kühlbrandt *et al.*, 1994), while the extrinsic proteins bound to the core part of PSII extend

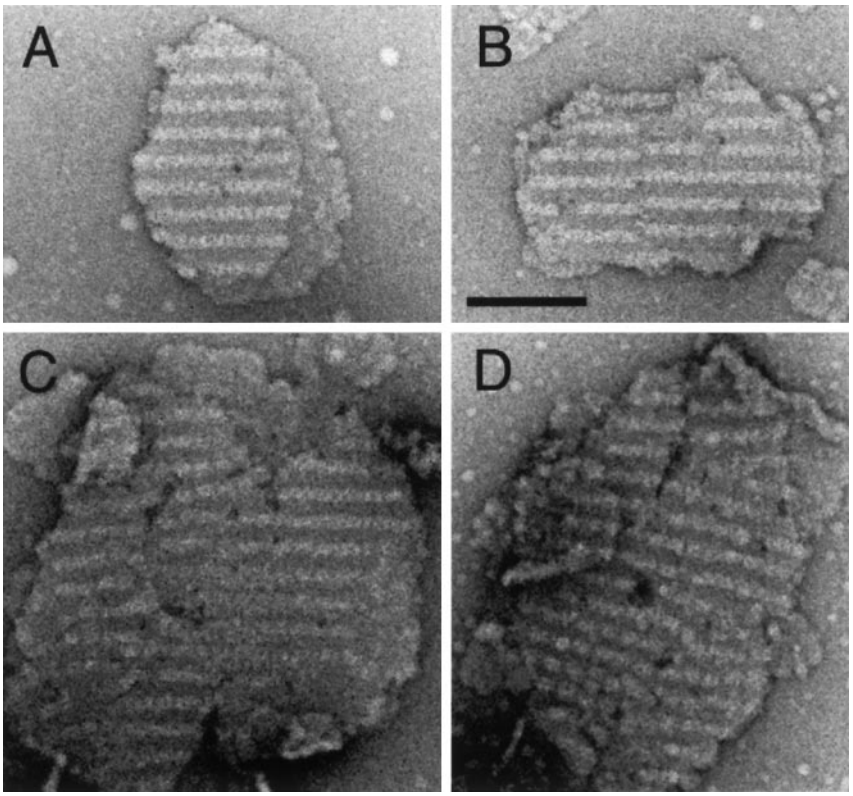

Figure 2. A gallery of paired inside-out grana membranes showing macrodomains in which PSII supercomplexes are in crystalline arrays with a spacing of 23 nm between the rows (small-spaced crystals). Fragments were negatively stained with 2% uranyl acetate. The space bar represents 100 nm.

up to 5 nm above the lumenal surface of the complex (e.g. see Nield *et al.*, 2000). This suggests that the extrinsic subunits of the core parts should contribute heavily to the most stain-excluding features of the projection maps and, since these units are located on the outside of the membranes (Dunahay *et al.*, 1984), two types of orientation are expected, mirror-related in projection. In the lower layer, the extrinsic subunits must face the carbon support film and, since this lower layer is usually somewhat more strongly contrasted by the negative stain, it is expected to dominate the analysis. This orientation is opposite to that of the single PSII-LHCII supercomplexes, which are predominantly (90 % or more) oriented with the extrinsic subunits away from the carbon support film (Boekema *et al.*, 1999a).

From a first examination of about 500 recorded paired grana membranes, it can be concluded that: (1) most, but certainly not all, membranes show macrodomains with a semi-crystalline lattice composed of rows of PSII core complexes in which the spacing between the rows is about 26.3 nm (Figure 1). The rows can, in principle, arise from both layers. If rows of both layers overlap, which occurs in only a minority of the images (see below), there are two preferential orientations. The rows in both layers either run in an almost parallel direction (Figure 1(a)) or they make an angle of roughly 40-50° (Figure 1(b)). From printed micrographs, the average angles were calculated to be 3(±4)° (S.D., $n = 17$) and 46(±10)° (S.D., $n = 26$) for the two types of orientations. (2) About 1 % of the membranes show macrodomains with a second type of crystalline lattice. The spacing between the rows is clearly smaller (23 nm) but, on average, these crystals are slightly better packed (Figure 2). (3) The amount of crystallinity is independent of the size of the membranes. There are large crystalline membranes (Figure 1(a)), as well as very small ones. In the larger paired membranes, several crystalline macrodomains can be present within one layer (Figure 1(a)); the angles between the domains were found to be rather random. Outside the crystalline macrodomains, the distribution of PSII is variable, but always lower on the average and even areas in paired membranes without any PSII in both layers were found (asterisks, Figure 1(a)). (4) The crystalline macrodomains are not stain-induced, because frozen-hydrated membranes show the same type of pattern, though with a much lower contrast (Figure 1(c)). Crystalline macrodomains were also visible in stacks of up to six membranes before detergent treatment (not shown). (5) In the small-spaced crystals, the striation pattern is much stronger, suggesting that the crystallinity is in both layers (Figure 2(a) and (b)). In the lower half of Figure 2(d), some individual core complexes can be distinguished, indicating less overlap. From both types of crystals, the best negatives were used for further image analysis.

Analysis of the macrodomains with the large-spaced crystalline arrays

In general, two superimposed crystalline lattices of two-dimensional crystals can be easily separated by making use of Fourier analysis, if the two layers differ in their rotational orientation. This is performed by masking off one of the two lattices in the two-dimensional Fourier transform. The two Fourier-filtered layers can then be used for additional steps in the analysis, because lattice imperfections can be corrected by cutting the crystals into fragments that undergo rotational and translational alignments using the Fourier-filtered layers as references (Saxton & Baumeister, 1982; Saxton *et al.*, 1992). These corrections can be done in real space and enable the contribution of the other layer to be erased from the total, just by summing aligned fragments of one layer. In the past, we followed this approach in the analysis of collapsed vesicle crystals of photosystem I (Böttcher *et al.*, 1992). However, the large-spaced crystalline arrays show such a strong disorder that it was impossible to achieve a Fourier-filtering from any of the crystals that could be used as a starting point for further analysis. Therefore, we analyzed the fragments as being single particles and started with the projection from the dimeric C_2S_2 supercomplex, derived from single-particle analysis (Boekema *et al.*, 1999a) as a first reference. With this reference, fragments were aligned and treated with multivariate statistical analysis and subsequently classified into 16 classes. The best class was used as a next reference and the whole procedure of alignments and classification was repeated four times. Class-sums from the final classification are presented in Figure 3; they show the same crystal pattern in two different ways. One type of orientation is represented by 13 class-sums, of which six are shown in Figure 3(a)-(e); the other type by only two (Figure 3(g) and (h)). The classification furthermore indicates the presence of some misaligned fragments (Figure 3(i)). The PSII core parts in classes A-E are mirror-related to those of the isolated PSII-LHCII supercomplexes (Boekema *et al.*, 1999a), which suggests that the PSII complexes in these classes are oriented with their lumenal sides towards the carbon support film (see above). The fact that more fragments align with these face-down complexes probably arises from the fact that the lower layer is usually somewhat more strongly contrasted by the negative stain.

From the best eight face-down classes, containing 1057 aligned fragments, the best 900 were summed, with the cross-correlation coefficient during the alignment step as the quality parameter (Figure 4(a)). The features of the strongly stain-excluding core parts indicate a unit cell with dimensions of 27.3 nm × 18.3 nm, and an angle of 74.5° between the axes. The characteristic rectangular shape of the dimeric C_2S_2 supercomplexes, which is dominated by the positions of the

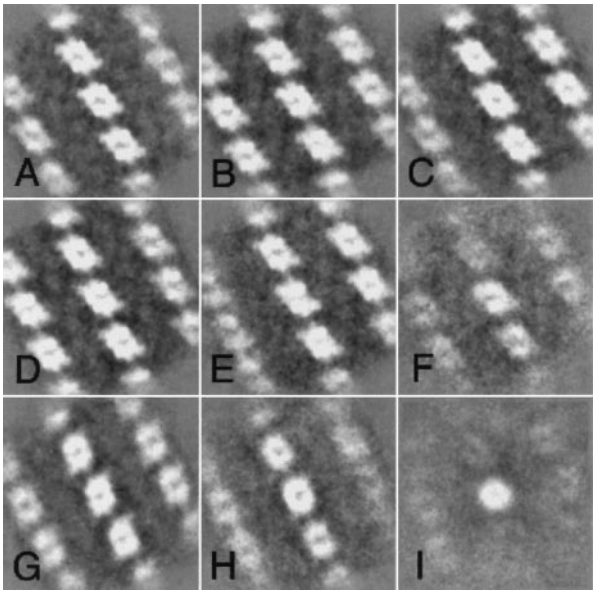

Figure 3. Image analysis of the large-spaced crystals. A set of 2303 aligned fragments was decomposed into 16 classes, of which nine are presented, after multivariate statistical analysis. The class-sums of (a)-(f) show averaged images of fragments with the crystal pattern from the lower membrane layer enhanced; the class-sums of (g) and (h) show the crystal pattern from the upper layer enhanced. (i) is a class-sum of mis-aligned fragments; seven classes similar to (a), (e) and (f) have been omitted from the presentation. The final class-sums are shown without symmetry imposed.

LHCII S trimer and CP26 (for a scheme, see Boekema *et al.*, 1999b) can be observed in these sums, as indicated in Figure 4(b). The dimensions of the C_2S_2 supercomplexes within the crystal fit well with the outlines as determined by the single-particle investigations (Boekema *et al.*, 1999a,b; Nield *et al.*, 2000), if the single particles are corrected for a boundary layer of attached detergent of 1.8 nm, as has been done in Figure 4(b). The C_2S_2 supercomplexes, however, do not completely occupy the crystal space and there remains considerable left-over space, as will be discussed below.

Analysis of the crystalline arrays with the small spacing

The membranes with the small-spaced crystalline macrodomains were analyzed in a way similar to that used for the large-spaced crystals; from 115 aligned fragments, the best 100 were summed (Figure 4(c)). The unit cell dimensions are 23 nm × 16.9 nm. Although the core part features are well defined and are similar to those of the large-spaced crystals, there is not much clear detail visible in the antenna region, possibly because the number of summed fragments was rather low. Nevertheless, the shape of the C_2S_2 supercomplexes from the single particle investigations can be fitted in and it can be seen that such supercomplexes fill the lattice quite well. These results indicate that the C_2S_2 supercomplex forms the basic unit of the crystal with the small spacing.

Analysis of positions of supercomplexes in the two superimposed layers

From the grana membrane fragment with the best preserved periodicity of the large-spaced crystal type, we analyzed how the individual PSII complexes are positioned (Figure 6). It will be relevant for a better understanding of the stacking process to know how the complexes in the two adjacent grana membranes are positioned with respect to each other. By correlation of individual PSII complexes with face-up and face-down oriented references, their positions in the two layers could be determined (marked by the black dots, Figure 6(b)). On these positions, rows of PSII complexes belonging to the lower membrane or upper membrane have been fitted (the blue and red core parts and the green and yellow contours of the PSII-LHCII supercomplexes in Figure 6(b)). If the molecules were first aligned to a reference with a handedness as in the lower layer and then to a reference with the different hand, which was first aligned on the first reference, several positions in the central part were shifted and rotated over a small but systematic angle ($5.6(\pm 2.7)^\circ$ (S.D., $n = 19$)), indicating that the correlation methods are accurate enough to systematically find the positions of individual molecules even if they are strongly overlapping.

The analysis suggests that a considerable part of the PSII core complexes do not have a PSII core counterpart in the other layer. In the upper three rows the detectable core complexes are all in a face-down orientation (the complexes depicted in blue, Figure 6(b)), in which the extrinsic subunits face the carbon support film, whereas in the lower three rows (the complexes depicted in red in Figure 6(b)) the complexes are in a face-up position. Only in the central layer, which has the strongest overall stain-excluding features (Figure 6(a)), there are many detectable PSII core complexes at both sides.

The well-ordered fragment of Figure 6 shows that the central rows of both layers run in a parallel direction with overlapping core parts. This is a frequently observed way of packing, but other organizations have been found in which the PSII core parts of the two layers are parallel but do not face each other (e.g. see the rows indicated by the two arrows in Figure 1(a)).

Discussion

Two types of semi-crystalline macrodomains

The image processing of the semi-crystalline arrays in the paired grana membrane fragments revealed two types of lattices. The first and most

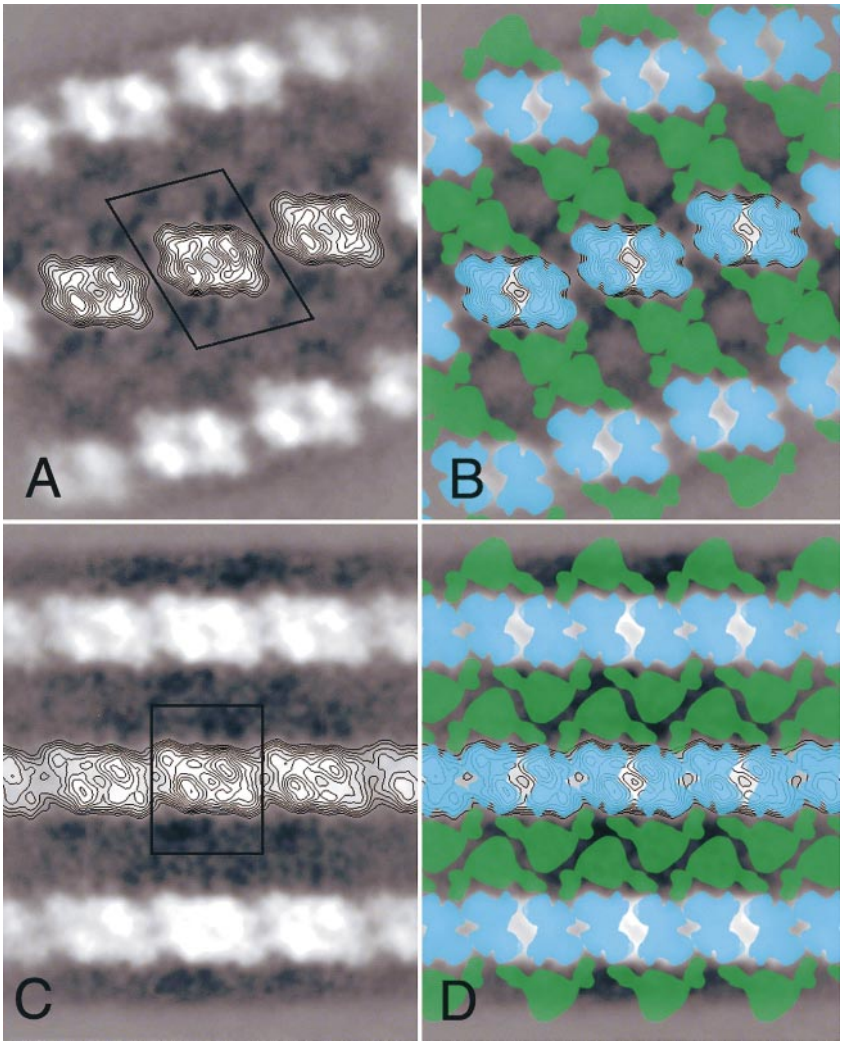

Figure 4. Final results of image analysis of the large-spaced and small-spaced crystals. (a) and (c) The sums of 900 and 100 fragments of both types of crystals. The unit cells of both crystal types are indicated. Images are presented in their mirror-versions, to facilitate comparison with all previously published supercomplex structures. In (b) and (d), supercomplexes of the C_2S_2 type have been fitted into the lattices, to indicate the position of the innermost part of the peripheral antenna (one S LHCII trimer plus one CP26 and one CP29 subunit; in green) around the dimeric core part (in blue).

abundant lattice has unit cell dimensions of 27.3 nm × 18.3 nm with an angle of 74.5° and a unit cell area of 481 nm^2. The second and minor lattice has a rectangular unit cell with dimensions of 23 nm × 16.9 nm and a unit cell area of 389 nm^2. Both crystal forms agree reasonably well with published data from electron microscopy. In a freeze-etch study of native thylakoid membranes from barley, large-spaced macrodomains with a similar crystalline packing and unit cell area (462 nm^2) were found (Simpson, 1978). In freeze-fractured membranes from *Pisum sativum* (Tageeva *et al*., 1978) a distance of 27.1 nm between the rows can be deduced for PSII complexes, compatible to a spacing of 26.3 nm for the rows in our large-spaced crystals. Bassi *et al*. (1989) analyzed and Fourier-filtered lattices from maize chloroplasts that had a rectangular unit cell of 26.7 nm × 17.8 nm. Lattices with dimensions similar to those of our small-spaced crystals have been observed quite often (e.g. see Miller, 1976; Seibert *et al*., 1987; Vallon *et al*., 1989; Marr *et al*., 1996; Lyon, 1998; Stoylova *et al*., 2000). Because some of these small-spaced and large-spaced lattices were obtained without any involvement of detergent, we suggest that both types of lattices represent native states of PSII arrangement in the thylakoid membrane. This suggestion is in agreement with the fact that the overall shape and diameter of the inside-out grana membranes and native membranes ara very similar (van Roon *et al*., 2000).

Fourier transformation of the final sums and evaluation of structure factors indicate that the resolution obtained by our image processing is about 2-2.5 nm for both crystal types and that only one type of lattice remained after aperiodic averaging. The enhanced lattices have sufficient detail to see the shape and handedness of the inner core parts of PSII supercomplexes directly, which can thus unambiguously be fitted into the lattices of the paired grana membranes. By doing so, the small-spaced lattice leaves just enough space to fit a C_2S_2 supercomplex. Especially in the direction along the striations, the supercomplexes come very close (Figure 4(c) and (d)). It is very likely that the similarly sized lattices observed before (see above) consist of C_2S_2 supercomplexes. This was already concluded from a crystal simulation of such lattices

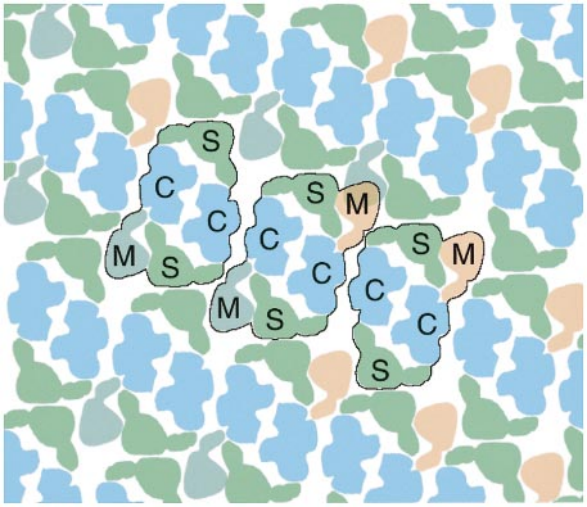

Figure 5. Possible ways of packing supercomplexes into the lattice of the large-spaced crystals. A symmetrical $C_2S_2M_2$ supercomplex, as outlined in the center, is too large to fit the lattice because of substantial overlap with M trimers of neighbouring supercomplexes, as indicated. This implies that only the smaller asymmetrical C_2S_2M complexes, in possible positions as indicated to the left and right of the $C_2S_2M_2$ supercomplex, can fit the lattice.

(Hankamer *et al.*, 1997b) and the unit cell dimensions of this hypothetical crystal are within a few per cent of the unit cell dimensions that were determined in this study, although the positioning of the supercomplexes differs.

The extra mass in the large-spaced crystals

The projection map of the large-spaced crystal analysis was obtained by imposing 2-fold rotational symmetry on the references used in the alignment step. Because previous work strongly indicates that the C_2S_2 supercomplex is always a dimer, imposing symmetry on the references was taken as a compromise to overcome the poor crystallinity of the large-spaced crystals as well as possible. In this way, the positions of the innermost S-type LHCII trimers flanking the dimeric core complex are clearly visible (Figure 4(a)). Without symmetry application, the features of the final projection map were less well defined, but not significantly different (not shown). A comparison with the single-particle projection maps shows that the positions of the S-type LHCII trimers are identical or highly similar (Boekema *et al.*, 1999a,b). It is the first time that these features of the supercomplex have been visualized within the membrane. The fitting of C_2S_2 supercomplexes within the lattice (Figure 4(b)) leaves no other conclusion than a building block of a C_2S_2 supercomplex and one or more additional proteins in the left-over space. This space is occupied by a density with an intensity very similar to that of the S-type LHCII trimers, far below that of the core parts. This rules out the possibility that this density is occupied by, for instance, the cytochrome *b*6/f complex, because this complex sticks out of the membrane at the lumenal side by at least 5 nm. This conclusion is in line with the biochemical analyses, which indicated that the cytochrome *b*6/f complex is not present in our grana membranes (van Roon *et al.*, 2000) and together these results demonstrate unequivocally that the cytochrome *b*6/f complex cannot be responsible for the additional mass in the large-spaced crystals.

Based on its level of intensity, which is similar to that of the S-type trimers, we consider it most likely that the extra mass is caused by LHCII complexes. The most obvious candidate is the M-type trimer (Boekema *et al.*, 1999a), perhaps together with one or two monomeric LHCII proteins. Figure 5 shows that a repeat of C_2S_2M particles fits the lattice rather well, but that a crystal motif of the larger $C_2S_2M_2$ particles is not possible because of excessive overlap with M trimers of neighbouring supercomplexes. An asymmetric C_2S_2M repeating unit could be one of the reasons for the overall considerable disorder of the crystallinity. For instance, it could be possible that within a domain some of the C_2S_2M particles differ by 180° from the others or that a few $C_2S_2M_2$ could slip in. This is not a totally irrelevant idea, since in the natural membrane stacking and destacking can occur within minutes, which also implies a mixing and demixing of components from the stacked membranes containing PSII with the unstacked membranes containing ATPase and PSI (see Anderson, 1999; Horton, 1999; and Garab & Mustardy, 1999).

The tentative attribution of the repeating unit of the large-spaced crystals as C_2S_2M implies that each unit should contain one CP24 protein (Boekema *et al.*, 1999a,b). However, it is clear that there is sufficient space for another protein with the mass of a monomeric LHCII protein. A suitable candidate is the PsbS protein, which is sometimes found in supercomplexes (Eshaghi *et al.*, 1999). Recent results have indicated that this PSII protein plays an essential role in the process of non-photochemical quenching (Li *et al.*, 2000), one of the most important regulation mechanisms in green plants (Horton, 1999).

Heterogeneity of supercomplexes and megacomplexes within one membrane

Our earlier research on isolated complexes obtained from partially solubilized PSII membranes indicated that some of the supercomplexes occurred in dimeric forms (Boekema *et al.*, 1999a,b). We found three types of these so-called megacomplexes. The first two types consisted of two $C_2S_2M_{1\text{-}2}$ units, whereas the third and least abundant type consisted of two C_2S_2 units. The only difference between the first two types was an approximately 7.5 nm lateral shift in the positions of the $C_2S_2M_{1\text{-}2}$ units. Based on the relative occur-

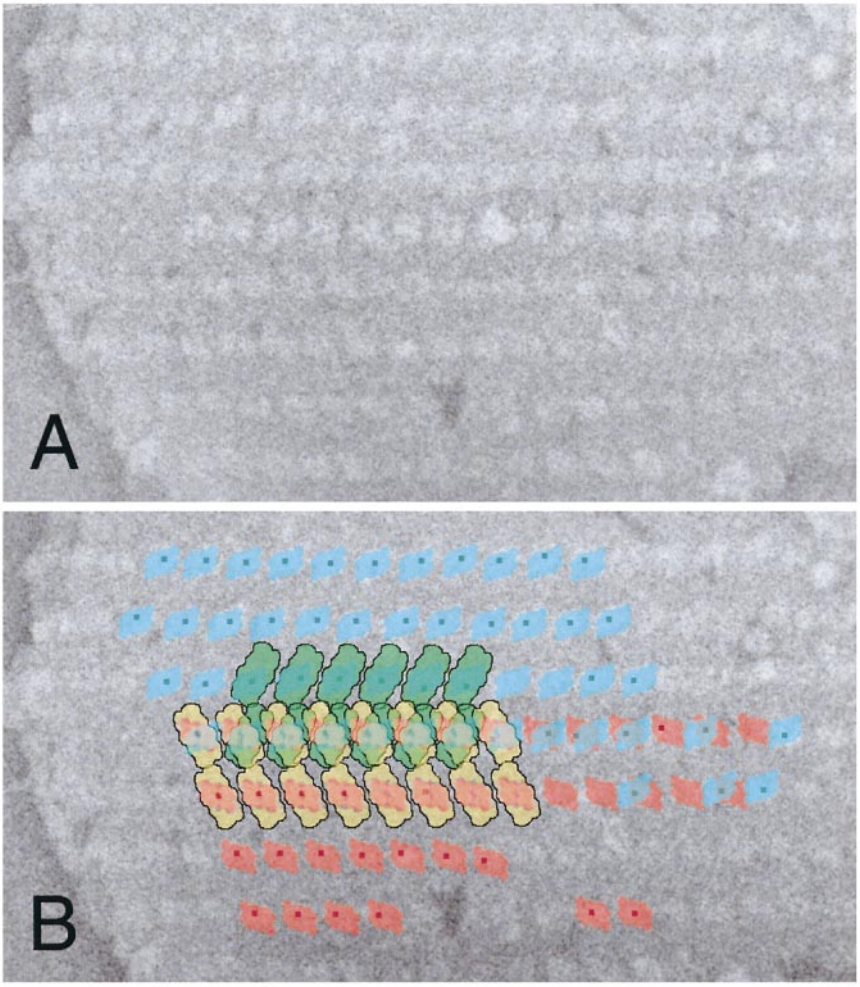

Figure 6. Analysis of positions of PSII supercomplexes in the two layers of paired membranes with large-spaced crystalline macrodomains that show a relatively high level of ordering of the PSII supercomplexes. The black dots indicate the positions of central supercomplexes in both layers as found by alignment procedures. On these positions, rows of PSII complexes belonging to the lower membrane (in blue) or upper membrane (in red) have been fitted. The inner part of the peripheral antenna of the supercomplexes is indicated in green and yellow, respectively.

rences of the megacomplexes in the various data sets and the very mild isolation procedure used, we suggested that these megacomplexes represent natural associations of PSII in the thylakoid membranes (Boekema *et al*., 1999a,b).

From a comparison between the various crystals and megacomplexes, it can be seen that there is a similarity between the large-spaced crystals and the most abundant (type I) megacomplex. If the crystals and the megacomplexes are positioned in the same orientation (with the extrinsic subunits upwards and with the long dimension of the supercomplexes along the *y*-axis), then each complex at the right side is shifted downwards by about 7.5 nm, both in the type I megacomplexes and in the large-spaced crystals. However, the distance between the two adjacent C_2S_2M units is about 1.5 nm longer in the type I megacomplexes (19.8 nm) than in the crystals (18.3 nm). From this discrepancy it becomes clear that these megacomplexes cannot be regarded as straightforward fragments of the large-spaced crystals.

The conclusion that the $C_2S_2M_2$ particles cannot fit the observed lattice may provide an explanation for the relatively low occurrence of solubilized $C_2S_2M_2$ supercomplexes (Boekema *et al*., 1999b). Analysis of a very large data set of supercomplexes revealed that the ratio of C_2S_2M to C_2S_2 was about 1:5, whereas that of $C_2S_2M_2$ to C_2S_2M was only about 1:15. It is possible that the type I and type II megacomplexes and the rare supercomplexes containing additional L-type trimers (Boekema *et al*., 1999a,b) are restricted to non-crystalline parts of membranes, but further work is required to establish the precise relationships between PSII arranged in crystalline and non-crystalline areas.

Relative positions of supercomplexes in adjacent layers

The results described here provide information on the relative positions of supercomplexes in the two adjacent layers. This question has been addressed before in freeze-fracture studies (Staehelin, 1975), but can be answered much more easily by electron microscopy using negatively stained specimens. It has been shown that the presence of bivalent cations is the main direct cause for the occurrence of stacked membranes, and that LHCII trimers are responsible for the major part of it (reviewed by Anderson, 1999). However, in mutant plants lacking LHCII, membrane stacking is not absent (Simpson, 1979) and isolated PSII supercomplexes have a strong tendency to stack upon standing (Boekema *et al.*, 1995). This indicates that PSII could be responsible. Analysis of a large number of micrographs made it clear that the orientation of the rows of adjacent layers is, to some extent, variable (although angles of about 0° and 45° between the rows seemed to predominate), and that therefore the interaction between PSII particles in the two membranes cannot be very specific.

The detailed analysis of the membranes in Figure 6 resulted in an unexpected observation: many PSII particles were found to have no PSII counterpart in the adjacent membrane. The lower membrane lattice predominates in the upper half of the crystalline macrodomain, whereas the upper membrane lattice is the main component of the lower half. Apparently, the remaining part of the superimposed membranes is rather smooth, and thus mostly occupied with LHCII, unbound to PSII supercomplexes.

The precise purpose of an organization with PSII-LHCII supercomplexes in one membrane and only LHCII in the adjacent part of the opposing layer is not entirely clear. The question is whether such an organization would provide an optimal harvesting of the excitation energy and thus whether all LHCII complexes would efficiently transfer the excitation energy to the photochemical reaction centers of PSII. If energy transfer takes place only by lateral movements within one membrane, then the presence of large LHCII-only domains in the membrane is not very favorable for efficient energy transfer. The average energy transfer kinetics between two LHCII trimers is probably about 30 ps (Van Grondelle *et al.*, 1994). If the LHCII-only domains have larger diameters than, for instance, 125 nm (as in the example of Figure 6) and if the average distance between two LHCII trimers is 8.3 nm (Dekker *et al.*, 1999), then many excitations will need at least 450 ps to reach a PSII reaction centre, which would be too slow for efficient energy transfer. It should be realized, however, that the distance between two adjacent rows is small (of the order of 2 nm, Nicolson, 1971) and that resonance energy transfer from one layer to the next by the Förster mechanism is quite possible. This means that the LHCII-only domains in one layer should be able to transfer excitation energy to the PSII complexes in the opposing layer. Experimental evidence for the occurrence of fast excitation energy transfer from one layer to the next has been provided by fast photovoltage experiments (Trissl *et al.*, 1987; Leibl *et al.*, 1989). These experiments revealed a lack of electrogenicity of PSII in stacked grana membranes and paired PSII membranes, but not in unstacked membranes and single PSII membranes. This lack was explained by an ''excitonic short-circuit'' between layers on a faster time-scale than the average time required for an excitation to reach the photoactive pigment of PSII in a single layer. Since this so-called trapping time is multiphasic and of the order of about 50-500 ps in intact PSII (discussed by Van Grondelle *et al.*, 1994), the excitation energy transfer from one layer to the next must occur in 50 ps or less.

The analysis of the paired membrane fragment shown in Figure 6 made it clear that in these particular two membranes the ratio of PSII to LHCII is about as expected from biochemical data (eight LHCII trimers per dimeric PSII core complex, Peter & Thornber, 1991). A calculation suggests that this fragment has a density of 1140-1190 dimeric core complexes per μm^2 within one layer. If the core complexes are considered to be all part of C_2S_2M supercomplexes, they would occupy about 55% of the overall membrane area. The remaining space could then accommodate five to six additional trimeric LHCII complexes, if the trimers have a packing efficiency compatible with the two-dimensional crystals of LHCII (Kühlbrandt *et al.*, 1994). We would like to point out, however, that this ratio may just be a coincidence, and that there may be also grana membranes with a considerably higher or lower LHCII content. For instance, some of our micrographs show grana membranes without much periodicity, but with many empty-PSII-areas, as indicated by the asterisks in Figure 1(a), indicating an abundance of trimeric/monomeric LHCII (see also Garab & Mustardy (1999) for LHCII-containing macrodomains). This suggests that the heterogeneity of PSII is restricted to the direct environment of the C_2S_2 supercomplexes (the presence or absence of one or two M and/or L types of LHCII trimers, and the presence or absence of monomeric LHCII proteins, Boekema *et al.*, 1999a,b), and to the complete macromolecular organization. It is possible that under certain physiological conditions other organizations may occur. An indication for this comes from an electron micrograph published by Cunningham & Crane (1966), which shows a nice semi-crystalline thylakoid membrane with a deduced lattice spacing of 34 nm. This is obviously outside the range of our large-spaced crystals. The fact that recognizable single Rubisco molecules with well-defined sizes are lying around the membranes excludes a simple magnification error in the presentation. Experiments with wild-type and mutant plants grown under controlled light conditions will be a logical

next step in further elucidating the overall grana membrane structure.

Materials and Methods

Isolation of inside-out grana membranes

Inside-out paired grana membranes were prepared from freshly isolated thylakoid membranes from spinach as described (van Roon *et al.*, 2000). In short, thylakoid membranes at a chlorophyll concentration of 1.4 mg/ml were suspended at 4 °C in a buffer containing 20 mM bis-Tris (pH 6.5) and 5 mM $MgCl_2$, solubilized with *n*-dodecyl-α,D-maltoside (α-DM, final concentration 1.2 %) during one minute and centrifuged for three minutes at 9000 rpm in a bench-top centrifuge, after which the supernatant was pushed through a 0.45 μm filter to remove large fragments and subjected to gel-filtration chromatography using a Superdex 200 HR 10/30 column (Pharmacia). The first green material that eluted from the column contained the grana membranes.

Electron microscopy and image analysis

Transmission electron microscopy was performed with a Philips CM10 electron microscope at 52,000× magnification. Negatively stained specimens were prepared with a 2% (w/v) solution of uranyl acetate on glow-discharged plain carbon-coated copper grids as described (Boekema *et al.*, 1999a) by diluting the inside-out grana sample 1:4 with buffer without α-DM. Unstained cryo-specimens were prepared using glow-discharged carbon films on 400-mesh copper grids. Grids were frozen in liquid ethane and transferred to a Gatan Cryoholder 626 for electron microscopy.

From 71 digitized negatives with macrodomains with large-spaced crystalline arrays, we selected 2303 partially overlapping fragments with a size of 144 pixels × 144 pixels (or 700 nm × 700 nm). From five negatives with macrodomains with small-spaced crystalline arrays 115 fragments of the same size (144 pixels × 144 pixels) were selected. Image analysis was carried out with IMAGIC software (Harauz *et al.*, 1988). The crystal fragments were analyzed following an aperiodic procedure, as for single particles, including repeated cycles of alignment procedures (Harauz *et al.*, 1988) and treatment by multivariate statistical analysis (Van Heel & Frank, 1981) and classification (Van Heel, 1989). The resolution of final sums was evaluated from the *IQ* values of structure factors obtained by 2D Fourier transformation according to Henderson *et al.* (1986).

Acknowledgements

We thank Dr W. Keegstra for his help with computer analysis and Mr K. Gilissen for technical support. Our research was supported, in part, by the Netherlands Foundation for Scientific Research (NWO) *via* the Foundation for Life and Earth Sciences (ALW).

References

Anderson, J. M. (1999). Insights in the consequences of grana stacking of thylakoid membranes in vascular plants: a personal perspective. *Aust. J. Plant Physiol.* **26**, 625-639.

Bassi, R., Ghiretti, Magaldi A., Tognon, G., Giacometti, G. & Miller, K. R. (1989). Two-dimensional crystals of the photosystem II reaction center complex from higher plants. *Eur. J. Cell Biol.* **50**, 84-93.

Berthold, D. A., Babcock, G. T. & Yocum, C. F. (1981). A highly resolved, oxygen-evolving photosystem II preparation from spinach thylakoid membranes. EPR and electron transport properties. *FEBS Letters,* **134**, 231-234.

Boekema, E. J., Hankamer, B., Bald, D., Kruip, J., Boonstra, A. F., Barber, J. & Rögner, M. (1995). Supramolecular structure of the photosystem II complex from green plants and cyanobacteria. *Proc. Natl Acad. Sci. USA,* **92**, 175-179.

Boekema, E. J., Nield, J., Hankamer, B. & Barber, J. (1998). Localization of the 23 kDa subunit of the oxygen evolving complex of photosystem II by electron microscopy. *Eur. J. Biochem.* **252**, 268-276.

Boekema, E. J., van Roon, H., Calkoen, F., Bassi, R. & Dekker, J. P. (1999a). Multiple types of association of photosystem II and its light-harvesting antenna in partially solubilized photosystem II membranes. *Biochemistry,* **38**, 2233-2239.

Boekema, E. J., van Roon, H., Van Breemen, J. F. L. & Dekker, J. P. (1999b). Supramolecular organization of photosystem II and its light-harvesting antenna in partially solubilized photosystem II membranes. *Eur. J. Biochem.* **266**, 444-452.

Böttcher, B., Gräber, P. & Boekema, E. J. (1992). The structure of photosystem I from the thermophilic cyanobacterium *Synechococcus* sp. determined by electron microscopy of two-dimensional crystals. *Biochim. Biophys. Acta,* **1100**, 125-136.

Cunningham, W. P. & Crane, F. L. (1966). Variation in membrane structure revealed by negative staining technique. *Expt. Cell Res.* **44**, 31-45.

Dekker, J. P., van Roon, H. & Boekema, E. J. (1999). Heptameric association of light-harvesting complex II trimers in partially solubilized photosystem II membranes. *FEBS Letters,* **449**, 211-214.

Dunahay, T. G., Staehelin, L. A., Seibert, M., Ogilvie, P. D. & Berg, S. P. (1984). Structural, biochemical and biophysical characterization of four oxygen-evolving photosystem II preparations from spinach. *Biochim. Biophys. Acta,* **764**, 179-193.

Eshaghi, S., Andersson, B. & Barber, J. (1999). Isolation of a highly active PSII-LHCII supercomplex from thylakoid membranes by a direct method. *FEBS Letters,* **446**, 23-26.

Garab, G. & Mustárdy, L. (1999). Role of LHCII-containing macrodomains in the structure, function and dynamics of grana. *Aust. J. Plant Physiol.* **26**, 649-658.

Hankamer, B., Barber, J. & Boekema, E. J. (1997a). Structure and membrane organization of photosystem II in green plants. *Annu. Rev. Plant Physiol. Plant Mol. Biol.* **48**, 641-671.

Hankamer, B., Nield, J., Zheleva, D., Boekema, E. J., Jansson, S. & Barber, J. (1997b). Isolation and biochemical characterisation of monomeric and dimeric photosystem II complexes from spinach and their relevance to the organisation of photosystem II *in vivo*. *Eur. J. Biochem.* **243**, 422-429.

Harauz, G., Boekema, E. & Van Heel, M. (1988). Statistical image analysis of electron micrographs of ribosomal subunits. *Methods Enzymol.* **164**, 35-49.

Henderson, R. J., Baldwin, J. M., Downing, K. H., Lepault, J. & Zemlin, F. (1986). Structure of purple membrane from *Halobacterium halobium*: recording, measurement and evaluation of electron micrographs at 3.5 Å resolution. *Ultramicroscopy,* **19**, 147-178.

Horton, P. (1999). Are grana necessary for regulation of light harvesting? *Aust. J. Plant Physiol.* **26**, 659-669.

Kühlbrandt, W., Wang, D. N. & Fujiyoshi, Y. (1994). Atomic model of plant light-harvesting complex by electron microscopy. *Nature,* **367**, 614-621.

Leibl, W., Breton, J., Deprez, J. & Trissl, H.-W. (1989). Photoelectric study on the kinetics of trapping and charge stabilization in oriented PS-II membranes. *Photosynth. Res.* **22**, 257-275.

Li, X.-P., Björkman, O., Shih, C., Grossman, A. R., Rosenquist, M., Jansson, S. & Niyogi, K. (2000). A pigment-binding protein essential for regulation of photosynthetic light harvesting. *Nature,* **403**, 391-395.

Lyon, M. K. (1998). Multiple crystal types reveal photosystem II to be a dimer. *Biochim. Biophys. Acta,* **1364**, 403-419.

Marr, K. M., McFeeters, R. L. & Lyon, M. K. (1996). Isolation and structural analysis of two-dimensional crystals of photosystem II from *Hordeum vulgare viridis zb63*. *J. Struct. Biol.* **117**, 86-98.

Miller, K. (1976). A particle spanning the photosynthetic membrane. *J. Ultrastruct. Res.* **54**, 159-167.

Nicolson, G. L. (1971). Structure of the photosynthetic apparatus in protein-embedded chloroplasts. *J. Cell Biol.* **50**, 258-263.

Nield, J., Orlova, E. V., Morris, E. P., Gowen, B., Van Heel, M. & Barber, J. (2000). 3D map of the plant photosystem II supercomplex obtained by cryoelectron microscopy and single particle analysis. *Nature Struct. Biol.* **7**, 44-47.

Peter, G. F. & Thornber, J. P. (1991). Biochemical composition and organization of higher plant Photosystem II light-harvesting pigment proteins. *J. Biol. Chem.* **266**, 16745-16754.

Rhee, K.-H., Morris, E. P., Barber, J. & Kühlbrandt, W. (1998). Three-dimensional structure of the plant photosystem II reaction centre at 8 Å resolution. *Nature,* **396**, 283-286.

Saxton, O. & Baumeister, W. (1982). The correlation averaging of a regularly arranged bacterial cell envelope protein. *J. Microsc.* **127**, 127-138.

Saxton, O., Durr, R. & Baumeister, W. (1992). From lattice distortion to molecular distortion: characterising and exploiting crystal deformation. *Ultramicroscopy,* **46**, 287-306.

Seibert, M., DeWit, M. & Staehelin, L. A. (1987). Structural localization of the O_2-evolving apparatus to multimeric (tetrameric) particles on the lumenal surface of freeze-etched photosynthetic membranes. *J. Cell Biol.* **105**, 2257-2265.

Simpson, D. J. (1978). Freeze-fracture studies on barley plastid membranes II. Wild-type chloroplast. *Carlsberg Res. Commun.* **43**, 365-389.

Simpson, D. J. (1979). Freeze-fracture studies on barley plastid membranes III. Location of the light-harvesting chlorophyll-protein. *Carlsberg Res. Commun.* **44**, 305-336.

Staehelin, L. A. (1975). Chloroplast membrane structure. Intramembranous particles of different sizes make contact in stacked membrane regions. *Biochim. Biophys. Acta,* **408**, 1-11.

Staehelin, L. A. (1976). Reversible particle movements associated with unstacking and restacking of chloroplast membranes *in vitro*. *J. Cell Biol.* **71**, 136-158.

Stoylova, S., Flint, T. D., Ford, R. C. & Holzenburg, A. (2000). Structural analysis of photosystem II in far-red-light-adapted thylakoid membranes. *Eur. J. Biochem.* **267**, 207-215.

Tageeva, S. V., Popov, V. I. & Allokhverdov, B. L. (1978). Complex electron microscopic study of structural and functional arrangement of chloroplast membranes. In *Proc. Ninth International Congress on Electron Microscopy, Toronto* (Sturgess, J. M., ed.), vol. 2, pp. 418-419, Imperial Press, Mississauga.

Trissl, H.-W., Breton, J., Deprez, J. & Leibl, W. (1987). Primary electrogenic reactions of Photosystem II as probed by the light-gradient method. *Biochim. Biophys. Acta,* **893**, 305-319.

Vallon, O., Tae, G-S., Cramer, W. A., Simpson, D., Hoyer-Hansen, G. & Bogorad, L. (1989). Visualization of antibody binding to the photosynthetic membrane: the transmembrane orientation of cytochrome *b*-559. *Biochim. Biophys. Acta,* **975**, 132-141.

Van Grondelle, R., Dekker, J. P., Gillbro, T. & Sundström, V. (1994). Energy transfer and trapping in photosynthesis. *Biochim. Biophys. Acta,* **1187**, 1-65.

Van Heel, M. (1989). Classification of very large electron microscopical image data sets. *Optik,* **82**, 114-126.

Van Heel, M. & Frank, J. (1981). Use of multivariate statistics in analysing images of biological macromolecules. *Ultramicroscopy,* **6**, 187-194.

Van Roon, H., Van Breemen, J. F. L., De Weerd, F. L., Dekker, J. P. & Boekema, E. J. (2000). Solubilization of green plant thylakoid membranes with *n*-dodecyl-α,D-maltoside. Implications for the structural organization of the photosystem II, photosystem I, ATP synthase and cytochrome *b*6/f complexes. *Photosynth. Res.* In the press.

Edited by M. F. Moody

(Received 10 March 2000; received in revised form 10 July 2000; accepted 17 July 2000)